Magnetic-field induced quantum-size cascades in superconducting nanowires

A. A. Shanenko,[1,2] M. D. Croitoru,[3] and F. M. Peeters[1]
[1]*TGM, Departement Fysica, Universiteit Antwerpen, B-2020 Antwerpen, Belgium*
[2]*Bogoliubov Laboratory of Theoretical Physics, Joint Institute for Nuclear Research, 141980 Dubna, Russia*
[3]*EMAT, Departement Fysica, Universiteit Antwerpen, B-2020 Antwerpen, Belgium*
(Received 3 June 2008; published 3 July 2008)

In high-quality nanowires, quantum confinement of the transverse electron motion splits the band of single-electron states in a series of subbands. This changes in a qualitative way the scenario of the magnetic-field induced superconductor-to-normal transition. We numerically solve the Bogoliubov-de Gennes equations for a clean metallic cylindrical nanowire at zero temperature in a parallel magnetic field and find that for diameters $D \lesssim 10$–15 nm, this transition occurs as a *cascade* of subsequent jumps in the order parameter (this is opposed to the smooth second-order phase transition in the mesoscopic regime). Each jump is associated with the depairing of electrons in one of the single-electron subbands. As a set of subbands contribute to the order parameter, the depairing process occurs as a cascade of jumps. We find pronounced quantum-size oscillations of the critical magnetic field with giant resonant enhancements. In addition to these orbital effects, the paramagnetic breakdown of Cooper pairing also contributes but only for smaller diameters, i.e., $D \lesssim 5$ nm.

DOI: 10.1103/PhysRevB.78.024505 PACS number(s): 74.78.Na

I. INTRODUCTION

High-quality superconducting nanostructures as, e.g., single-crystal Sn nanowires,[1] polycrystalline (but made of strongly coupled grains) Al nanowires,[2,3] and single-crystalline atomically uniform Pb nanofilms[4–7] have recently been fabricated. It was possible to minimize the disorder such that the electron mean free path was about or larger than the specimen thickness.[2,3,7] In this case the scattering on nonmagnetic imperfections influences only the electron motion parallel to the wire/film, while the perpendicular electron motion is governed by the transverse-size quantization. Indeed, photoemission spectra of ultrathin single-crystal Pb films showed clear signatures of the splitting of the electron band into a series of subbands due to the transverse-size quantization.[4] In the presence of minimal disorder the so-called Anderson theorem[8] (see, also, discussion in Ref. 9) controls the effect of nonmagnetic impurities. Thus, one can expect that the study of a clean system with quantized transverse electron motion can capture important issues concerning the impact of quantum confinement on the superconducting characteristics in high-quality nanowires/nanofilms.

The single-electron subbands appearing due to the transverse quantization move in energy with changing specimen thickness. When the bottom of a subband passes through the Fermi surface, the density of single-electron states at the Fermi level increases abruptly. This results in size-dependent superconducting resonances[10] and in quantum-size oscillations of the superconducting properties as function of the thickness. Recently such quantum-size oscillations in the critical temperature T_c of superconducting Pb nanofilms were observed at a high level of experimental precision and sophistication.[4,5] Quantum-size superconducting resonances were shown to be responsible for an increase in the superconducting transition temperature in Al and Sn nanowires with decreasing thickness.[11]

The transverse quantization of the electron motion should strongly influence the superconducting-to-normal phase transition driven by a magnetic field in such high-quality nanowires/nanofilms. In the present paper we limit ourselves to nanowires in a parallel magnetic field and ignore the vortex formation because vortices cannot nucleate in very thin superconducting wires.

According to the Ginzburg-Landau (GL) theory,[12,13] the critical magnetic field is expected to increase as $1/D$ in the Meissner state, with D the diameter of the mesoscopic wire. Furthermore, the superconducting-to-normal phase transition in a magnetic field is of second order for such mesoscopic wires while being of first order in bulk (for type I superconductors).[8] It is a general characteristic of the GL theory that this transition becomes of second order in mesoscopic specimens.[8,14] Recent calculations based on the Bogoliubov-de Gennes (BdG) equations[15] for wires with diameters 20–200 nm confirmed the GL result and revealed a smooth superconducting-to-normal transition in a parallel magnetic field at any temperature below T_c. This is in agreement with recent experimental data on Sn[1,16] and Zn[17] nanorods. Hence, one may conclude that effects of the transverse quantization of the electron motion are not significant for metallic superconducting wires with width larger than 20 nm.

In the present paper we show that the situation changes dramatically for smaller widths. Our analysis is based on a numerical self-consistent solution of the BdG equations for a clean cylindrical metallic nanowire. We predict that at zero temperature the superconducting-to-normal transition driven by a magnetic field parallel to the nanowire, occurs as a *cascade* of jumps in the order parameter (with clear signatures of hysteretic behavior) for diameters $D \lesssim 10$–15 nm. This qualitative change is accompanied by pronounced quantum-size oscillations of the critical magnetic field with large enhancements at the points of the superconducting resonances. In addition to these orbital effects, we found that Pauli paramagnetism can also contribute but its role is only significant for smaller diameters, i.e., $D \lesssim 5$ nm.

II. BOGOLIUBOV-DE GENNES EQUATIONS

In the clean limit the BdG equations[8] read

$$E_n u_n(\mathbf{r}) = \hat{H}_e u_n(\mathbf{r}) + \Delta(\mathbf{r}) v_n(\mathbf{r}), \tag{1a}$$

$$E_n v_n(\mathbf{r}) = \Delta^*(\mathbf{r}) u_n(\mathbf{r}) - \hat{H}_e^* v_n(\mathbf{r}), \tag{1b}$$

where $\Delta(\mathbf{r})$ stands for the superconducting order parameter ($*$ for complex conjugate), E_n is the quasiparticle energy, $u_n(\mathbf{r})$ and $v_n(\mathbf{r})$ are the particlelike and holelike wave functions. The single-electron Hamiltonian appearing in Eqs. (1a) and (1b) is given by

$$\hat{H}_e = \frac{1}{2m_e}\left(-i\hbar\nabla - \frac{e}{c}\mathbf{A}\right)^2 - E_F, \tag{2}$$

with m_e the electron band mass (can be set to the free-electron mass without loss of generality), and E_F the Fermi level. The BdG should be solved in a self-consistent manner, together with the self-consistency relation

$$\Delta(\mathbf{r}) = g\sum_n u_n(\mathbf{r}) v_n^*(\mathbf{r})(1-2f_n), \tag{3}$$

with g the coupling constant and $f_n=f(E_n)$ the Fermi function.[8]

An important issue is the range of the states included in the sum in Eq. (3). The usual prescription concerns the quasiparticles with positive energies E_n. At the same time the corresponding single-electron energy ξ_n should be located in the Debye window, $|\xi_n|<\hbar\omega_D$ with ω_D the Debye frequency and

$$\xi_n = \int d^3r[u_n^*(\mathbf{r})\hat{H}_e u_n(\mathbf{r}) + v_n^*(\mathbf{r})\hat{H}_e v_n(\mathbf{r})]. \tag{4}$$

However, in the presence of a magnetic field, this prescription is modified: $\hat{H}_e|_{\mathbf{A}=0}$ is used rather than $\hat{H}_e$ in Eq. (4). It is well known that the selection $|\xi_n|<\hbar\omega_D$ appears as a result of the delta-function approximation for the effective electron-electron interaction. Such an approximation neglects a complex structure of the Fourier transform of the pair interaction. The problem is cured by the well-known cutoff in *the canonical-momentum* space. Such a cutoff results in the above selection rule for ξ_n with $\hat{H}_e$ replaced by $\hat{H}_e|_{\mathbf{A}=0}$ (see, for instance, Refs. 8 and 15). Second, the requirement of positive quasiparticle energies has to be weakened in the presence of a magnetic field. Namely, one needs to include the states having positive quasiparticle energies only at zero magnetic field. This allows one to investigate also the regime of gapless superconductivity when the presence of quasiparticles with negative energies manifests the depairing reconstruction of the ground state [see Eq. (9) below and Appendix].

Due to transverse quantum confinement we set

$$u_n(\mathbf{r})|_{\mathbf{r}\in S} = v_n(\mathbf{r})|_{\mathbf{r}\in S} = 0 \tag{5}$$

on the wire surface. Periodic boundary conditions are used along the nanowire. Screening of the external magnetic field can be neglected for narrow wires. Then, for a constant magnetic field parallel to the nanocylinder, $H_\parallel$, it is convenient to use the well-known Coulomb gauge. Thus, for cylindrical wires we have $\Delta(\mathbf{r})=\Delta(\rho)$ with ρ,φ,z the cylindrical coordinates (below the order parameter is chosen as a real quantity). The set of relevant quantum numbers is $n=\{j,m,k\}$, with j the quantum number associated with ρ, m the azimuthal quantum number, and k the wave vector of the quasifree electron motion along the nanowire. In this case the particlelike and holelike wave functions can be represented as

$$u_n(\mathbf{r}) = u_{jmk}(\rho)\frac{e^{im\varphi}}{\sqrt{2\pi}}\frac{e^{ikz}}{\sqrt{L}}, \tag{6a}$$

$$v_n(\mathbf{r}) = v_{jmk}(\rho)\frac{e^{im\varphi}}{\sqrt{2\pi}}\frac{e^{ikz}}{\sqrt{L}}, \tag{6b}$$

with L the length of the nanowire. Inserting Eqs. (6a) and (6b) into the BdG Eqs. (1a) and (1b) and using an expansion in terms of the Bessel functions (see details in Ref. 18), the problem is reduced to the diagonalization of a matrix.

III. DISCUSSION OF NUMERICAL RESULTS

A. Resonances in the critical magnetic field

At a superconducting resonance the main contribution to the different superconducting quantities comes from the subband (or subbands) whose bottom passes through the Fermi surface. For cylindrical wires, the subbands with the same $|m|$ are degenerate for $H_\parallel=0$ and, hence, any size-dependent resonant enhancement of the order parameter (e.g., the energy gap and the critical temperature) can be specified by the set $(j,|m|)$ in the absence of a magnetic field. Due to quantum-size oscillations in the pair-condensation energy, we get corresponding oscillations in the critical magnetic field whose resonant enhancements can also be labeled by $(j,|m|)$. Figure 1(a) shows the critical field $H_{c,\parallel}$ calculated self-consistently from Eqs. (1a) and (1b) at zero temperature ($T=0$) for an aluminum nanocylinder with diameter D. Note that $H_{c,\parallel}$ is set as the magnetic field above which the spatially averaged order parameter $\bar{\Delta}$ drops below $0.01\Delta_{\text{bulk}}$, with Δ_{bulk} the bulk gap. Here, we consider as an example Al and take[8] $\hbar\omega_D=32.31$ meV and $gN(0)=0.18$, where $N(0)$ stands for the bulk density of states. For this choice $\Delta_{\text{bulk}}=0.25$ meV. The effective Fermi level is set to $E_F=0.9$ eV, which is used together with the BdG equations within the parabolic band approximation.[19] As seen, $H_{c,\parallel}$ exhibits huge enhancements as compared to the bulk critical magnetic field $H_{c,\text{bulk}}=0.01$ T (to simplify our discussion, we show first the results for extremely narrow quantum wires). Resonances in $H_{c,\parallel}$ are found to be very dependent on D and $|m|$. The states with large $|m|$ are more strongly influenced by $H_\parallel$ and, so, the resonances in $H_{c,\parallel}$ governed by large $|m|$ are, as a rule, less pronounced. In contrast, the resonances controlled by $m=0$ are very stable. For instance, a superconducting solution to Eqs. (1a) and (1b) exists at $D=1.94$ nm [the resonance associated with $(j,|m|)=(1,0)$] even for an abnormally large magnetic field of about 1000 T. Similar behavior is found for

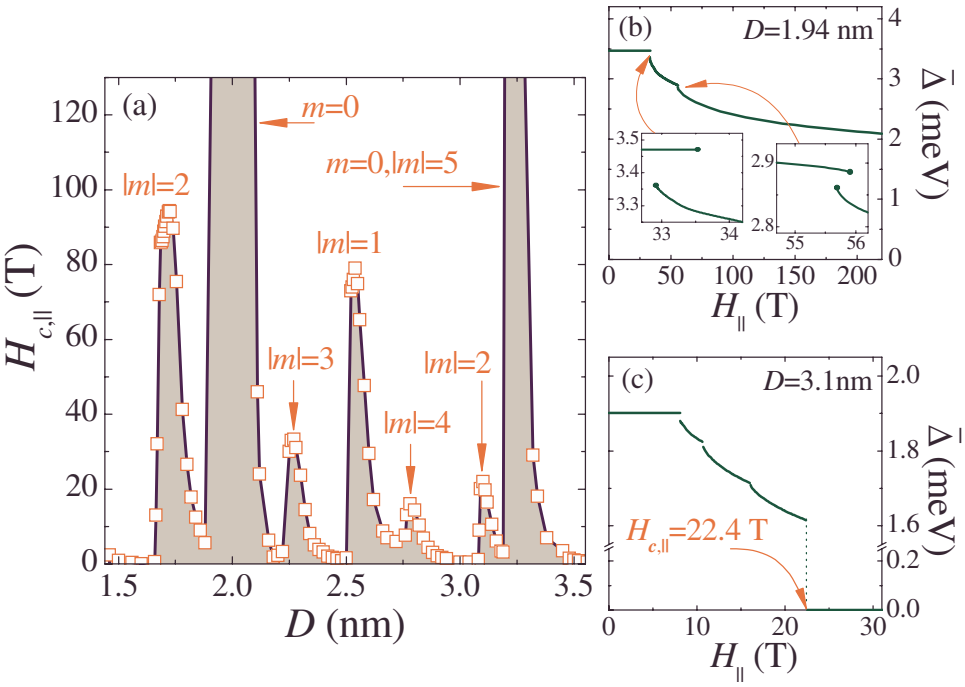

FIG. 1. (Color online) (a) Critical parallel magnetic field $H_{c,\|}$ versus the nanowire diameter D, and spatially averaged order parameter $\bar{\Delta}$ as function of $H_\|$ for the resonant diameters (b) $D=1.94$ nm [governed by $(j,|m|)=(1,0)$] and (c) $D=3.1$ nm [governed by $(j,|m|)=(1,2)$].

the resonance at $D=3.21$ nm with $(j,m)=(2,0)$. Note that in Fig. 1 two neighboring resonances with $(j,m)=(2,0)$ [$D=3.21$ nm] and $(j,|m|)=(1,5)$ [$D=3.28$ nm] merge and result in one profound increase in $H_{c,\|}$.

B. Quantum-size cascades

Figures 1(b) and 1(c) show two typical examples ($m=0$ and $|m|\neq 0$) of how the spatially averaged order parameter $\bar{\Delta}$ depends on $H_\|$. To discuss these results, we remark that the quasiparticle energies can be well approximated by

$$E_{jmk}=\sqrt{\xi_{jmk}^2+\Delta_{jmk}^2}-m\mu_B H_\|, \tag{7}$$

where ξ_{jmk} is the single-electron energy given by Eq. (4) (at $H_\|=0$), μ_B stands for the Bohr magneton, and

$$\Delta_{jmk}=\int_0^R d\rho\rho\Delta(\rho)[|u_{jmk}(\rho)|^2+|v_{jmk}(\rho)|^2], \tag{8}$$

the averaged value of the order parameter as seen by jmk quasiparticles ($R=D/2$). Equation (8) can be derived within Anderson's approximate solution of the BdG equations.[20] This approximate solution implies that the particlelike and holelike wave functions are chosen to be proportional to the eigenfunctions of $\hat{H}_e$ (for details, see Appendix). Note that the dependence of Δ_{jmk} on k is found to be negligible: $\Delta_{jmk}=\Delta_{jm}$ [see Eq. (A6)]. As follows from Eq. (7), quasiparticles with $m>0$ are moved down in energy by $H_\|$. Each time when a quasiparticle branch specified by a positive m touches zero, a jump in $\bar{\Delta}$ occurs. When a branch controlling a resonant enhancement approaches zero, $\bar{\Delta}$ jumps down to zero and the superconducting solution disappears [see Fig. 1(c)]. Other quasiparticle branches are less important (due to a smaller density of states) and are responsible for small (sometimes almost insignificant) jumps in $\bar{\Delta}$. In particular, at $D=1.94$ nm the first small jump in $\bar{\Delta}$ [see Fig. 1(b)] is located at $H_\|=33.5$ T. Here the branch with $j=0,m=2$ touches zero (see Fig. 2). The insets in Fig. 1(b) show details of jumps in $\bar{\Delta}$. As seen, there are clear signatures of hysteretic behavior: in the vicinity of any jump, the BdG equations have two possible solutions.

To properly clarify details of the hysteretic behavior, we performed a numerical analysis for sufficiently large values of the unit-cell length L, controlling periodic boundary conditions in the longitudinal direction. In particular, the limit $L\to\infty$ can be approached only when $L>10$–20 μm ($L/D>10^5$). For $m=0$ the last term in Eq. (7) is "switched off" and so $\bar{\Delta}$ exhibits only a sequence of small jumps for the resonances governed by $m=0$ [see Fig. 1(b)]. For any quasiparticle branch an energy gap $\Delta_E^{(jm)}$ (see Fig. 2) can be introduced, and the total excitation energy gap is defined as $\Delta_E=\min\Delta_E^{(jm)}$. Stress that in general, $\Delta_{jm}\neq\Delta_E^{(jm)}$, only at $H_\|=0$ we have $\Delta_E=\min\Delta_{jm}$. Thus, a jump in $\bar{\Delta}$ appears when one of $\Delta_E^{(jm)}$ becomes zero. In particular, the left-side inset in Fig. 1(b) shows that there exist two solutions in the interval from $H_\|=32.94$ T to $H_\|=33.5$ T (the first jump in the order parameter as a function of $H_\|$). For the upper solution we have $\Delta_E=\Delta_{0,2}\geq 0$ that decreases linearly with $H_\|$ until touching zero at $H_\|=33.5$ T [see the quasiparticle energies corresponding to the upper solution and given in Figs. 2(a) and 2(b) for $H_\|=0$ and $H_\|=33.5$ T, respectively]. For the lower solution $\Delta_E^{(0,2)}=0$ and so the gapless regime is realized with

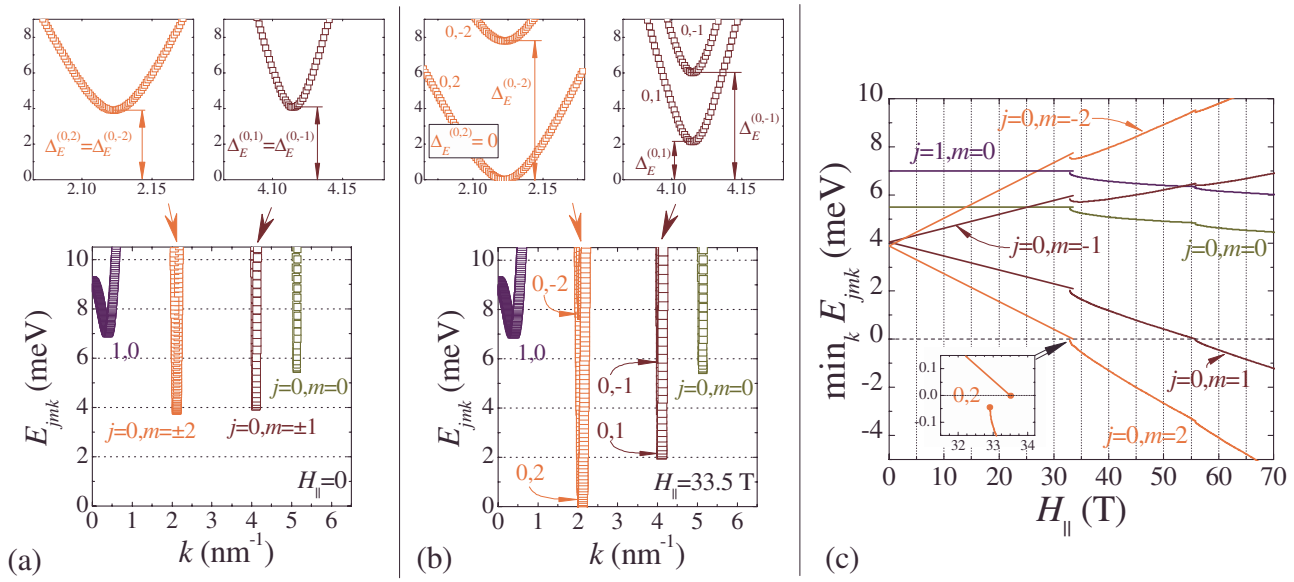

FIG. 2. (Color online) The quasiparticle energies E_{jmk} versus k for the four relevant branches $(j,m)=(0,0),(0,\pm1),(0,\pm2)$ and (1,0) at (a) $H_\parallel=0$ and (b) $H_\parallel=33.5$ T for the resonant diameter $D=1.94$ nm. In this case there are two nonzero solutions of the BdG equations for 32.9 T$\leq H_\parallel \leq$33.5 T [see the left-side inset in Fig. 1(b)], the upper one disappears at $H_\parallel=33.5$ T [panel (b)] when the quasiparticle branch (0,2) touches zero. (c) The quantity $\min_{\mathbf{k}} E_{jmk}$ versus $H_\parallel$ for the different quasiparticle branches at $D=1.94$ nm.

$\Delta_E=\Delta_E^{(0,2)}=0$. For more detail, Fig. 2(c) shows how $\min_{\mathbf{k}} E_{jmk}$ varies with $H_\parallel$ for $D=1.94$ nm. As seen, each relevant quasiparticle branch exhibits signatures of two small jumps [corresponding to the jumps in the order parameter given in Fig. 2(b)]. After the first jump $\min_{\mathbf{k}} E_{0,2,k}<0$ (see the inset) and so $\Delta_E^{(0,2)}=0$. After the second jump (for $H_\parallel>55.85$ T) $\min_{\mathbf{k}} E_{0,1,k}$ becomes negative and, hence, we get $\Delta_E=\Delta_E^{(0,1)}=\Delta_E^{(0,2)}=0$. In the near vicinity of the second jump, for 55.7 T$\leq H_\parallel \leq$55.85 T, we again find two nonzero solutions for the BdG equations: $\Delta_E^{(0,1)}\neq 0$ for the upper solution (except of the edge point $H_\parallel=55.85$ nm) and $\Delta_E^{(0,1)}=0$ for the lower one. Above, we discussed only numerical results for the resonances. The same conclusions hold for the off-resonant points. However, the eventual jump to zero in $\bar{\Delta}$ at $H_\parallel=H_{c,\parallel}$ is, of course, much less pronounced in this case.

Now the question arises: *what is the physics underlying these cascades of jumps in the order parameter?* A jump appears when one of the relevant quasiparticle branches touches zero. From this point on, such a branch "supplies" the system with states having negative quasiparticle energies [see the discussion about Eq. (3) in Sec. II]. For such quasiparticles $f_n=1$ at zero temperature or, in other words, these quasiparticles survive even at $T=0$. It means that we face a reconstruction of the ground state. To have a feeling about such a reconstruction, let us consider the multiband Bardeen-Cooper-Schrieffer (BCS) ansatz for the ground-state wave function [see Appendix, Eq. (A9)]. This ansatz reads

$$|\Psi\rangle = \prod_{j,m,k} (U_{jmk}^* - V_{jmk}^* a_{j,m,k\uparrow}^\dagger a_{j,-m,-k\downarrow}^\dagger)|0\rangle, \tag{9}$$

where $a_{j,m,k\uparrow}^\dagger(a_{j,m,k\uparrow})$ is the creation (annihilation) operator for electrons in the state j,m,k with the z spin projection $\uparrow$, and U_{jmk} and V_{jmk} are given by

$$U_{jmk} = \int \mathrm{d}^3 r \varphi_{jmk}^*(\mathbf{r}) u_{jmk}(\mathbf{r}), \tag{10a}$$

$$V_{jmk} = \int \mathrm{d}^3 r \varphi_{jmk}^*(\mathbf{r}) v_{jmk}(\mathbf{r}), \tag{10b}$$

with $\varphi_{jmk}(\mathbf{r})$ being the eigenfunction of $\hat{H}_e$ [the term $\propto \mathbf{A}^2(\mathbf{r})$ can be neglected, see, for instance, Ref. 15],

$$\varphi_{jmk}(\mathbf{r}) = \sqrt{\frac{2}{R}} J_m\left(\frac{\alpha_{jm}}{R}\rho\right) \frac{e^{im\varphi}}{\sqrt{2\pi}} \frac{e^{ikz}}{\sqrt{L}}, \tag{11}$$

where $J_m(x)$ is the mth order Bessel function, and α_{jm} is its jth zero. When a quasiparticle with a negative energy appears at $T=0$ (say, with the quantum numbers $j',m',k',\uparrow$), the ground state given by Eq. (9) should be abandoned in favor of

$$\gamma_{j',m',k',\uparrow}^\dagger |\Psi\rangle = a_{j',m',k',\uparrow}^\dagger \prod_{\substack{jmk\neq \\ j'm'k'}} (U_{jmk}^* - V_{jmk}^* a_{j,m,k,\uparrow}^\dagger a_{j,-m,-k,\downarrow}^\dagger)|0\rangle, \tag{12}$$

where $\gamma_{j',m',k',\uparrow}^\dagger$ stands for the quasiparticle creation operator,

$$\gamma_{j',m',k',\uparrow}^\dagger = U_{j'm'k'} a_{j',m',k'\uparrow}^\dagger + V_{j'm'k'} a_{j',-m',-k',\downarrow}.$$

As seen, Eq. (12) differs from Eq. (9) due to the sector j',m',k': in Eq. (12) we simply have the single-electron creation operator rather than the Cooper-pair correlation term including the product $a_{j,m,k,\uparrow}^\dagger a_{j,-m-k,\downarrow}^\dagger$. Therefore, the reconstruction mentioned above is due to the depairing of electrons. For instance, as seen from Figs. 2(b) and 2(c), the quasiparticle branch with $j=0,m=2$ touches zero at $H_\parallel=33.5$ T and, at higher magnetic fields, acquires negative

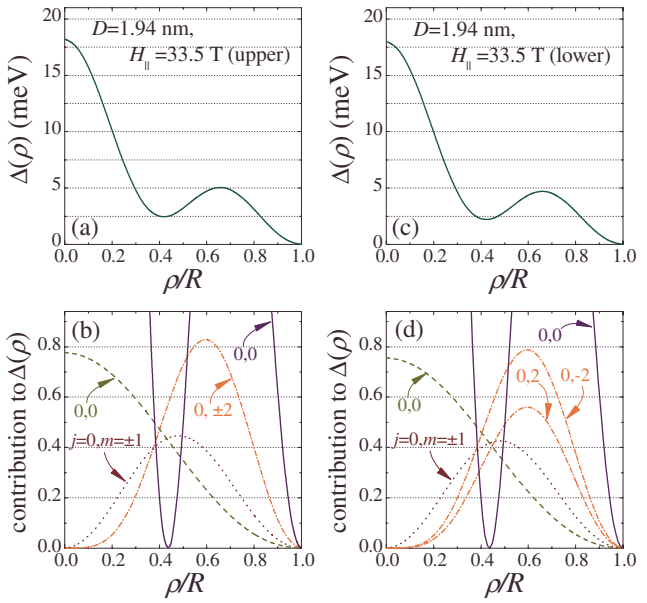

FIG. 3. (Color online) The upper [(a), (b)] and lower [(c), (d)] solutions of the BdG equations at $H_{\|}=33.5$ T (the resonant diameter $D=1.94$ nm): (a) and (c), the order parameter $\Delta(\rho)$; (b) and (d), the corresponding contribution of the different relevant single-electron subbands.

energies. This gives rise to the depairing of electrons in the single-electron subband $j=0,m=2$, which results in the drop of the order parameter [see the left-side inset in Fig. 1(b)]. Note that such a drop occurs not only due to a decay of the Cooper pairs in the subband $j=0,m=2$. Throughout the self-consistency relation [Eq. (3)], such a decay influences and reduces the contributions of all other subbands. However, the binding energies of the Cooper pairs in these subbands are somewhat reduced rather than the depairing of electrons occurs. In Fig. 3 the order parameter is plotted together with the contributions of different single-electron subbands for the upper [Figs. 3(a) and 3(b)] and lower [Figs. 3(c) and 3(d)] solutions of the BdG equations at $H_{\|}=33.5$ T and $D=1.94$ nm. Comparing panels (a) and (c), we find that the order parameter decreases slightly by a few percent, which results in a small jump of $\bar{\Delta}$ in Fig. 1(b) (the left-side inset). From Figs. 3(b) and 3(d), we can see that all the subband contributions are also reduced by a few percent when passing from the upper to the lower solution, except for $j=0,m=2$. For $j=0,m=2$ we have a significant drop by a factor of 1.5, which is a manifestation of electron depairing. In a quasi-one-dimensional system there is a set of single-electron subbands contributing to the order parameter, and so the depairing process occurs as *a quantum-size cascade of jumps*.

C. Effect of thickness

In the previous subsection, for the sake of simplicity, we considered extremely small diameters. So the question arises about the effect of thickness. In Fig. 4(a) $\bar{\Delta}$ is plotted as a function of $H_{\|}$ and D for larger diameters, i.e., $D=4$–6 nm. We see that the quantum-size oscillations in $H_{c,\|}$ are correlated (as to the positions of the resonances) with the corresponding oscillations in $\bar{\Delta}$. However, contrary to the $\bar{\Delta}$ resonances, amplitudes of resonant enhancements in $H_{c,\|}$ are mainly determined by $|m|$. The most profound increases in $H_{c,\|}$ correspond to $m=0$ and appear at $D=4.55$ and 5.9 nm. Signatures of jumps in $\bar{\Delta}$ can again be observed [see, also, the contour plot given in Fig. 4(b)]. For instance, at $D=4.22$ nm the averaged order parameter $\bar{\Delta}$ jumps from a value about 2 meV down to zero at $H_{\|}=H_{c,\|}=6$ T. At $D=4.77$ nm a jump of about 1 meV occurs at $H_{\|}=H_{c,\|}=4$ T. For the off-resonant values of D we also have jumps in $\bar{\Delta}$ but less pronounced. Note that the resonant enhancements in the superconducting condensate governed by $j=3,m=0$ and $j=4,m=0$ are very stable against $H_{\|}$ but decay significantly faster as compared to the situation of smaller diameters.

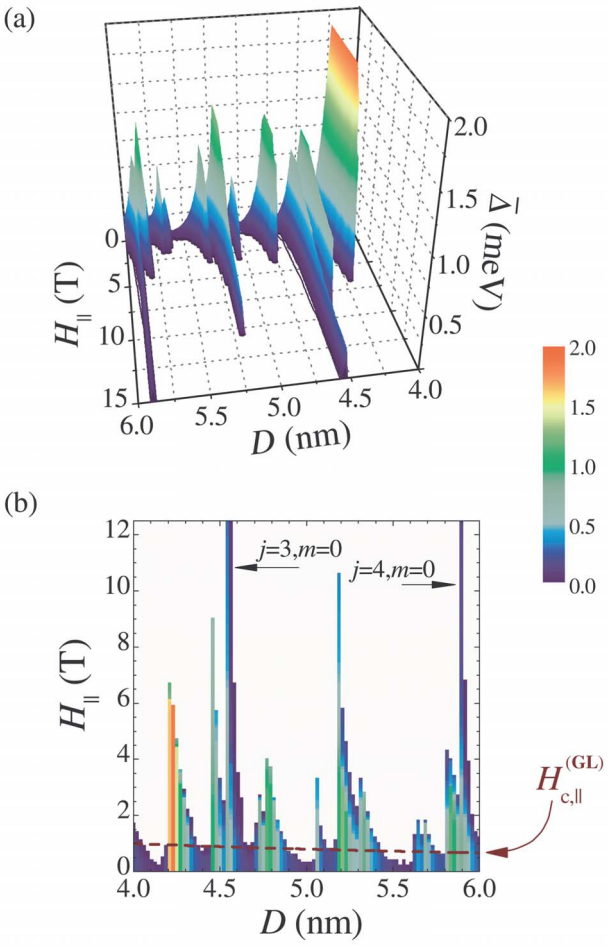

FIG. 4. (Color online) (a) Averaged order parameter $\bar{\Delta}$ as a function of $H_{\|}$ and D for diameters 4–6 nm and (b) the contour plot of this function. The dashed curve in (b) shows the GL result for the critical magnetic field.

The number of relevant single-electron subbands scales as $\propto D^2$, which results in complex patterns of the hysteretic behavior accompanying the jumps in $\bar{\Delta}$ at larger diameters. An example of such a complex pattern is shown in Fig. 5, where details of the first jump in $\bar{\Delta}(H_{\|})$ are given for $D=4.26$ nm (the half-decay point of the resonance appearing at $D=4.22$ nm). In this case there are two hysteretic loops. The

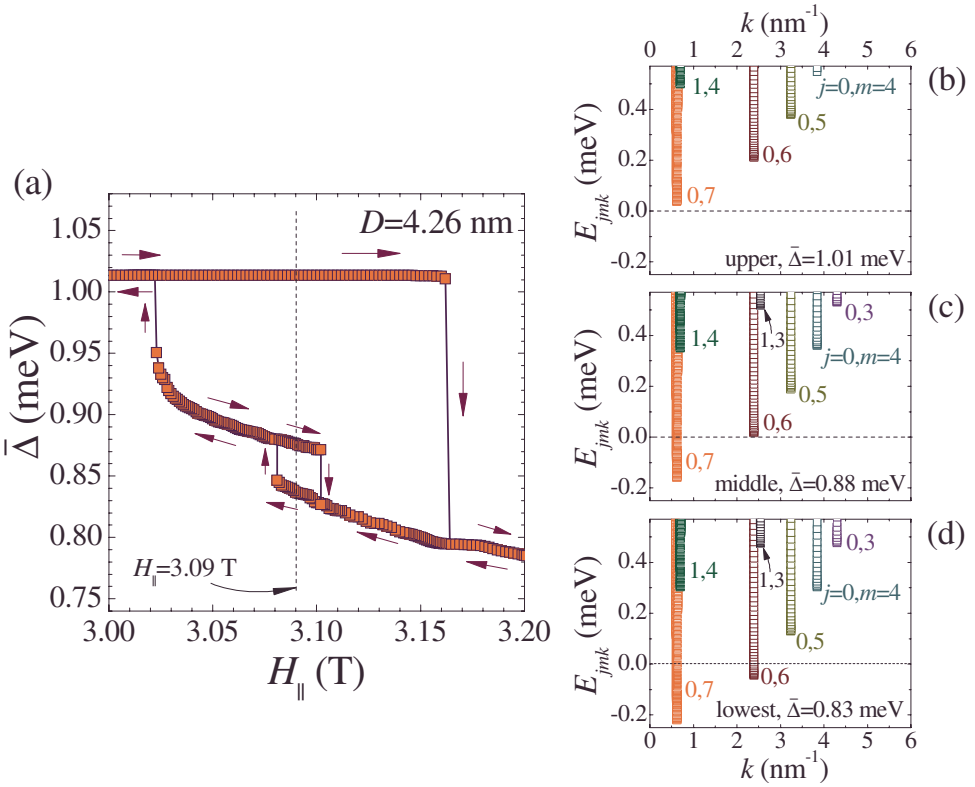

FIG. 5. (Color online) (a) Multihysteretic behavior at the first jump in $\bar{\Delta}$ as a function of $H_{\parallel}$ for $D=4.26$ nm, and the lowest quasiparticle energies for three solutions of the BdG equations at $H_{\parallel}=3.09$ T: (b) the upper with $\bar{\Delta}=1.01$ meV, (c) the middle with $\bar{\Delta}=0.88$ meV, and (d) the lower with $\bar{\Delta}=0.83$ meV.

larger loop is realized for $3.02\ \mathrm{T}<H_{\parallel}<3.16\ \mathrm{T}$ [see panel (a)]. Surprisingly, it includes a smaller hysteretic loop arising for $3.08\ \mathrm{T}<H_{\parallel}<3.1\ \mathrm{T}$. In this magnetic-field range there exist three solutions of the BdG equations. Low-lying quasiparticle energies for each of these solutions are given in Figs. 5(b)–5(d) for $H_{\parallel}=3.09$ T. As seen, all the quasiparticle energies are positive for the upper solution [panel (b)], which is the gap regime and $\Delta_E=\Delta_{0,7}>0$. For the middle solution [panel (c)] we have $\min_{\mathbf{k}} E_{0,7,k}<0$, and so $\Delta_{0,7}=0$. This is a signature of the depairing of electrons in the subband with $j=0,m=7$. For the lowest solution [panel (d)] the decay of the Cooper pairs occurs in the two single-electron subbands with the quantum numbers $j=0,m=7$ and $j=0,m=6$. For both the middle and lowest solution negative quasiparticle, energies make a contribution to the problem, which is typical of the gapless regime.

Note that the GL theory is not able to give the found quantum-size cascades and the quantum-size oscillations in the critical magnetic field (due to the absence of quantum confinement in the GL formalism). When using a simplified estimate based on the GL formula[12,13] $H_{c,\parallel}^{(GL)}=8.0\lambda H_{c,\mathrm{bulk}}/D$ (with λ the magnetic penetration depth) together with the zero-temperature expectations $\lambda\approx 50$ nm and $H_c=0.01$ T for Al in the clean limit[8]), we obtain the dashed curve in Fig. 4(b), which gives roughly the averaged trend for $H_{c,\parallel}$ found with the BdG formalism.

For thicker mesoscopic wires with $D>20$ nm, the role of any given quasiparticle branch becomes much less significant, and quantum-size oscillations in the superconducting properties are strongly reduced. In this regime we recover the smooth superconducting-to-normal transition, in agreement with the previous theoretical results[15] and recent experimental observations.[1,17,21]

D. Pauli paramagnetism

We remark that in the current approach we neglected Pauli paramagnetism entirely and included only orbital effects. This is justified when the paramagnetic (Pauli) limiting field[22]

$$H_P=\frac{\Delta_E(H=0)}{\sqrt{2}\mu_B}$$

is larger than the orbital values of $H_{c,\parallel}$ (note that $\bar{\Delta}\approx\Delta_E$ at zero magnetic field). From Fig. 4(b) one can estimate that $H_P\approx 23$ T (12, 14, 16, 11, 9, and 14 T) versus $H_{c,\parallel}\approx 6$ T (9, 4, 11, 3, 2, and 4 T) at $D=4.22$ nm (4.45, 4.77, 5.2, 5.33, 5.68, and 5.85 nm). As seen, Pauli paramagnetism is only crucial for the resonances governed by $m=0$, i.e., at $D=4.55$ and 5.88 nm, and it can produce some minor corrections to the resonances governed by $|m|=1$ (see, for instance, $D=5.2$ nm) and by $|m|=2$ (see, for example, $D=4.45$ nm). However, most of the resonant enhancements for $D>5$ nm are produced by the states with $|m|>2$ (the larger the diameter, the smaller the relative number of resonances labeled by $|m|\leq 2$).

Thus, our numerical results are not very sensitive to the spin-magnetic interaction for $D>5$ nm, whereas signatures

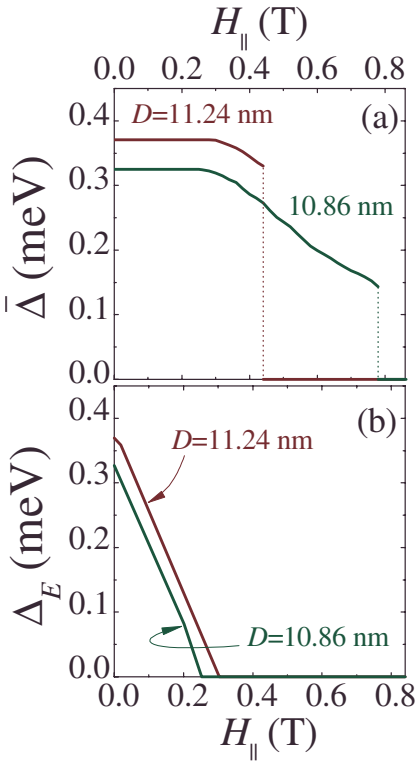

FIG. 6. (Color online) (a) Spatially averaged order parameter $\bar{\Delta}$ and (b) the energy gap Δ_E versus $H_\parallel$ for the resonant diameters $D=10.86$ nm and $D=11.24$ nm.

of jumps in $\bar{\Delta}$ are observed up to $D\approx 10$–15 nm. In particular, Fig. 6 shows $\bar{\Delta}$ [Fig. 6(a)] and Δ_E [Fig. 6(b)] versus $H_\parallel$ at $D=10.86$ nm ($H_P=3.9$ T) and $D=11.24$ nm ($H_P=4.5$ T). The energy gap decays as a set of lines with different slopes, which reflects the linear dependence of E_{jmk} on $H_\parallel$ in Eq. (7). It is remarkable that only jumps to zero in $\bar{\Delta}$ are clearly seen in Fig. 6(a): a cascade of preceding small jumps has nearly collapsed into a continuous curve.

IV. CONCLUDING REMARKS

The quantization of the transverse electron motion in high-quality nanowires results in the splitting of the single-electron band into a series of subbands. Based on a numerical solution of the Bogoliubov-de Gennes equations for a clean metallic nanocylinder, we showed that such a splitting leads to important qualitative changes in the interplay of superconductivity and magnetic field in nanowires with diameters $\lesssim$10–15 nm. At zero temperature the superconducting-to-normal transition driven by a parallel magnetic field occurs as a cascade of jumps in the order parameter (a second-order phase transition is realized for mesoscopic wires). At the same time the critical magnetic field exhibits quantum-size oscillations with pronounced resonant enhancements.

Our results are for nanowires with uniform cross section along the wire. Real samples will exhibit inevitable cross-section fluctuations that will smooth the quantum-size oscillations of superconducting properties, resulting in an overall enhancement with decreasing thickness [for $H_{c,\parallel}$ this enhancement can follow the simple estimate based on the GL theory, see Fig. 3(b)]. Such a monotonical increase in T_c has recently been found in Al and Sn nanowires.[11] At present, the parallel critical magnetic field has been measured in Sn (Refs. 1 and 21) and Zn (Ref. 17) wires with diameters down to 20 nm. These nanowires were found to be still in the mesoscopic regime. It is expected that data on $H_{c,\parallel}$ for $D<20$ nm will be available in the near future.

Note that, on the qualitative level, our results are not sensitive to the specific confining geometry; the only thing that is of importance is the formation of the single-electron subbands. Thus, the same conclusions should hold for superconducting high-quality films (but not for nanograins where the orbital effects are known to be negligible, see, for instance, Refs. 23 and 24). It is well known[25,26] that for ultrathin films the paramagnetic breakdown of the Cooper pairing results in a first-order superconducting-to-normal transition driven by a parallel magnetic field (provided that the effect of the spin-orbital scattering is not very significant and the temperature is close to zero). We expect that the quantum-size cascades can precede this paramagnetic breakdown. Fluctuations in thickness can somewhat destroy the cascades, and so atomically uniform high-quality nanofilms can be quite good to observe the orbital effects predicted in this paper.

ACKNOWLEDGMENTS

The authors thank D. Y. Vodolazov for stimulating discussions. This work was supported by the Flemish Science Foundation (FWO-Vl), the Interuniversity Attraction Poles Programme, Belgian State, Belgian Science Policy (IAP), the ESF-AQDJJ network, and BOF-TOP (University of Antwerpen).

APPENDIX: ANDERSON'S APPROXIMATE SOLUTION

To have an idea about the validity of Eqs. (7) and (8), it is instructive to consider Anderson's approximate solution to the BdG equations.[20] The main assumption is that $u_n(\mathbf{r})$ and $v_n(\mathbf{r})$ are proportional to the eigenfunction of $\hat{H}_e$ given by Eq. (11) [the term $\propto \mathbf{A}^2(\mathbf{r})$ in $\hat{H}_e$ can be ignored],

$$u_n(\mathbf{r}) = U_n\varphi_n(\mathbf{r}), \quad v_n(\mathbf{r}) = V_n\varphi_n(\mathbf{r}), \tag{A1}$$

with $n=\{j,m,k\}$. Note that U_{jmk} and V_{jmk} are the same as in Eqs. (10a) and (10b). Inserting Eqs. (A1) into Eqs. (1a) and (1b), we recast the BdG equations into

$$E_{jmk}U_{jmk} = [\xi_{jmk} - \mu_B m H_\parallel]U_{jmk} + \Delta_{jmk}V_{jmk}, \tag{A2a}$$

$$E_{jmk}V_{jmk} = \Delta^*_{jmk}U_{jmk} - [\xi_{jmk} + \mu_B m H_\parallel]V_{jmk}, \tag{A2b}$$

where $\Delta_{jmk}=\Delta^*_{jmk}$ (the order parameter is chosen as real) is given by Eq. (8), μ_B stands for the Bohr magneton, and ξ_{jmk} [the single-electron energy at $H_\parallel=0$, see the discussion next to Eq. (4)] is of the form

$$\xi_{jmk} = \frac{\hbar^2}{2m_e}\left[\frac{\alpha^2_{jm}}{R^2} + k^2\right] - E_F, \tag{A3}$$

with α_{jm} the jth zero of the mth order Bessel function.

Equations (A2a) and (A2b) have a nontrivial solution only when the relevant determinant is zero,

$$\begin{vmatrix} E_{jmk} - \xi_{jmk} + \mu_B m H_\parallel & -\Delta_{jmk} \\ -\Delta_{jmk} & E_{jmk} + \xi_{jmk} + \mu_B m H_\parallel \end{vmatrix} = 0,$$

which leads to

$$E_{jmk} = \pm \sqrt{\xi_{jmk}^2 + \Delta_{jmk}^2} - \mu_B m H_\parallel, \tag{A4}$$

where the + sign corresponds to the physical solution. This explains Eq. (7) used for the interpretations of our numerical results in Sec. III. Taking into account the normalization condition (U_{jmk} and V_{jmk} are real)

$$U_{jmk}^2 + V_{jmk}^2 = 1, \tag{A5}$$

together with Eqs. (8) and (A1), one can find that Δ_{jmk} does not depend on k [see our discussion after Eq. (8)],

$$\Delta_{jmk} = \Delta_{jm} = \frac{2}{R}\int_0^R \mathrm{d}\rho\rho J_m^2\left(\frac{\alpha_{jm}}{R}\rho\right)\Delta(\rho). \tag{A6}$$

Now, for a given Δ_{jm}, Eqs. (A2a) and (A2b) can be solved analytically, which results in (for the physical E_{jmk})

$$U_{jmk}^2 = \frac{1}{2}\left(1 + \frac{\xi_{jmk}}{\sqrt{\xi_{jmk}^2 + \Delta_{jm}^2}}\right), \tag{A7a}$$

$$V_{jmk}^2 = \frac{1}{2}\left(1 - \frac{\xi_{jmk}}{\sqrt{\xi_{jmk}^2 + \Delta_{jm}^2}}\right), \tag{A7b}$$

$$U_{jmk}V_{jmk} = \frac{\Delta_{jm}}{2\sqrt{\xi_{jmk}^2 + \Delta_{jm}^2}}. \tag{A7c}$$

It is worth noting that the magnetic field is not present explicitly in Eqs. (A7a) and (A7b), and U_{jmk} and V_{jmk} depend on $H_\parallel$ only through Δ_{jm}. Equations (A1), (A7a), and (A7b) make it possible to rewrite Eq. (3) in the form of the following BCS-like self-consistency equation:

$$\Delta_{j'm'} = -\sum_{jmk} V_{j'm',jm}\frac{\Delta_{jm}\tanh(\beta E_{jmk}/2)}{2\sqrt{\xi_{jmk}^2 + \Delta_{jm}^2}}, \tag{A8}$$

with β the inverse temperature and the pair-interaction matrix element

$$V_{j'm',jm} = -\frac{2g}{\pi R^2 L}\int_0^R \mathrm{d}\rho\rho J_{m'}^2\left(\frac{\alpha_{j'm'}}{R}\rho\right)J_m^2\left(\frac{\alpha_{jm}}{R}\rho\right).$$

The summation in Eq. (A8) is over the physical states with ξ_{jmk} being in the Debye window, $|\xi_{jmk}| < \hbar\omega_D$.

Note that Eqs. (A1) is exact only when $\Delta(\rho)=\text{const}$, which is not the case in the presence of quantum confinement. However, one can expect that Anderson's approximation is good enough when the Cooper pairing of electrons from different subbands is negligible, i.e., for narrow wires with a strong impact of the transverse quantization. This expectation is in agreement with our numerical results revealing that Anderson's approximation is accurate within a few percent when $D < 5$–10 nm. In particular, according to Eq. (A8), the superconducting order parameter is constant at zero temperature until quasiparticles with negative energies appear: $\tanh(\beta E/2) \to 1$ for $\beta \to \infty$ when $E > 0$, whereas $\tanh(\beta E/2) \to -1$ in the opposite case. This explains why $\bar{\Delta}$ given in Figs. 1, 5, and 6 is practically independent of $H_\parallel$ before the gapless regime.

As mentioned above, Anderson's solution is a good approximation when the Cooper-pairing of electrons from different subbands plays a minor role. So, Anderson's prescription given by Eq. (A1) is equivalent to the multiband BCS model whose Hamiltonian can be written as ($n=\{j,m,k\}$)

$$\hat{H} = \sum_n \sum_\sigma (\xi_n - \mu_B m H_\parallel) a_{n\sigma}^\dagger a_{n\sigma} + \frac{1}{2}\sum_{nn'}\sum_\sigma V_{jm,j'm'} a_{n\sigma}^\dagger a_{\bar{n}-\sigma}^\dagger a_{\bar{n}'-\sigma} a_{n'\sigma}, \tag{A9}$$

with $\bar{n}=\{j,-m,-k\}$ and σ the electron spin projection. Comparing Eq. (A9) with the bulk-reduced BCS Hamiltonian, one can easily generalize the well-known BSC ansatz for the bulk ground-state wave function to the multiband ansatz given by Eq. (9) in Sec. III.

[1] M. L. Tian, J. G. Wang, J. Snyder, J. Kurtz, Y. Liu, P. Schiffer, T. E. Mallouk, and M. H. W. Chan, Appl. Phys. Lett. **83**, 1620 (2003); M. Tian, J. Wang, J. S. Kurtz, Y. Liu, M. H. W. Chan, T. S. Mayer, and T. E. Mallouk, Phys. Rev. B **71**, 104521 (2005).

[2] M. Zgirski, K.-P. Riikonen, V. Touboltsev, and K. Arutyunov, Nano Lett. **5**, 1029 (2005).

[3] F. Altomare, A. M. Chang, M. R. Melloch, Y. Hong, and C. W. Tu, Phys. Rev. Lett. **97**, 017001 (2006).

[4] Y. Guo, Y.-F. Zhang, X.-Y. Bao, T.-Z. Han, Z. Tang, L.-X. Zhang, W.-G. Zhu, E. G. Wang, Q. Niu, Z. Q. Qiu, J.-F. Jia, Z.-X. Zhao, and Q. K. Xue, Science **306**, 1915 (2004).

[5] D. Eom, S. Qin, M.-Y. Chou, and C. K. Shih, Phys. Rev. Lett. **96**, 027005 (2006).

[6] M. M. Özer, J. R. Thompson, and H. H. Weitering, Nat. Phys. **2**, 173 (2006).

[7] M. M. Özer, J. R. Thompson, and H. H. Weitering, Phys. Rev. B **74**, 235427 (2006).

[8] P. G. de Gennes, *Superconductivity of Metals and Alloys* (Benjamin, New York, 1966).

[9] M. A. Skvortsov and M. V. Feigel'man, Phys. Rev. Lett. **95**, 057002 (2005).

[10] J. M. Blatt and C. J. Thompson, Phys. Rev. Lett. **10**, 332 (1963).

[11] A. A. Shanenko, M. D. Croitoru, M. Zgirski, F. M. Peeters, and K. Arutyunov, Phys. Rev. B **74**, 052502 (2006).

[12] V. P. Silin, Zh. Eksp. Teor. Fiz. **21**, 1330 (1951) (in Russian).

[13] O. S. Lutes, Phys. Rev. **105**, 1451 (1957).

[14] V. A. Schweigert and F. M. Peeters, Phys. Rev. B **57**, 13817 (1998).
[15] J. E. Han and V. H. Crespi, Phys. Rev. B **69**, 214526 (2004).
[16] L. Jankovič, D. Gournis, P. N. Trikalitis, I. Arfaoui, T. Cren, P. Rudolf, M.-H. Sage, T. T. M. Palstra, B. Kooi, J. De Hosson, M. A. Karakassides, K. Dimos, A. Moukarika, and T. Bakas, Nano Lett. **6**, 1131 (2006).
[17] J. S. Kurtz, R. R. Johnson, M. Tian, N. Kumar, Z. Ma, S. Xu, and M. H. W. Chan, Phys. Rev. Lett. **98**, 247001 (2007).
[18] A. A. Shanenko and M. D. Croitoru, Phys. Rev. B **73**, 012510 (2006).
[19] A. A. Shanenko, M. D. Croitoru, and F. M. Peeters, Europhys. Lett. **76**, 498 (2006); A. A. Shanenko, M. D. Croitoru, and F. M. Peeters, Phys. Rev. B **75**, 014519 (2007).
[20] P. W. Anderson, J. Phys. Chem. Solids **11**, 26 (1959).
[21] T. G. Sorop and L. J. de Jongh, Phys. Rev. B **75**, 014510 (2007).
[22] D. Saint-James, G. Sarma, and E. J. Thomas, *Type II Superconductivity* (Pergamon, New York, 1969).
[23] J. von Delft, Ann. Phys. **10**, 219 (2001).
[24] V. N. Gladilin, V. M. Fomin, and J. T. Devreese, Phys. Rev. B **70**, 144506 (2004).
[25] K. Maki, Phys. Rev. **148**, 362 (1966).
[26] P. M. Tedrow, R. Meservey, and B. B. Schwartz, Phys. Rev. Lett. **24**, 1004 (1970).